Artificial neural network to predict the chemical composition-dependence of stacking fault energy in austenitic stainless steels

Red neuronal artificial para predecir la dependencia a la composición química de la energía de falla de apilamiento en aceros inoxidables austeníticos

Alfonso M. Román[2], Bernardo Campillo[2,3], Arturo Molina[1], Horacio Martínez[2], Itzel Reyes[3], Osvaldo Flores[2]

[1]Centro de Investigación en Ingeniería y Ciencias Aplicadas, UAEM, México.
[2]Instituto de Ciencias Físicas, UNAM, México.
[3]Facultad de Química, UNAM, México

*Correo-e: alfonso.romans@uaem.edu.mx

PALABRAS CLAVE:

Artificial Neural network, stacking fault energy, austenitic stainless steel.

RESUMEN

Stacking fault energy (SFE) is an important parameter to be considered in the design of austenitic stainless steels (SS) due to its influence on magnetic susceptibility, atomic order changes and intergranular corrosion resistance. An extensive review of specialized literature was examined in order to understand the different methods that have been developed for the calculation of SFE. Characterization by transmission electron microscopy (TEM), linear expressions from data processing and first-principles quantum mechanics approximations are some techniques that have been used for the calculation of SFE. In the present work a feed forward backpropagation artificial neural network (ANN) was developed to predict the SFE within given specific ranges of chemical compositions for austenitic SS. The experimental data were extracted from a research work reported by Yonezawa et al [1], and then were analyzed for three different heat treatment conditions. The present model predicts SFE values with a correlation coefficient of 0.99, which is a minor error when is compared with other works in the literature.

KEYWORDS:

Artificial Neural network, stacking fault energy, austenitic stainless steel.

ABSTRACT

Stacking fault energy (SFE) is an important parameter to be considered in the design of austenitic stainless steels (SS) due to its influence on magnetic susceptibility, atomic order changes and intergranular corrosion resistance. An extensive review of specialized literature was examined in order to understand the different methods that have been developed for the calculation of SFE. Characterization by transmission electron microscopy (TEM), linear expressions from data processing and first-principles quantum mechanics approximations are some techniques that have been used for the calculation of SFE. In the present work a feed forward backpropagation artificial neural network (ANN) was developed to predict the SFE within given specific ranges of chemical compositions for austenitic SS. The experimental data were extracted from a research work reported by Yonezawa et al [1], and then were analyzed for three different heat treatment conditions. The present model predicts SFE values with a correlation coefficient of 0.99, which is a minor error when is compared with other works in the literature.

Recibido: 25 de mayo de 2018 • **Aceptado:** 2 de marzo de 2020 • **Publicado en línea:** 30 de junio de 2020

1. INTRODUCTION

Stacking represents the way in which the layers of atoms are found in the crystal lattice. Stacking faults are areas that have different crystal structure from the original. Therefore, stacking faults appear in FCC crystal when the sequence ABCABCABC ... of stacking of compact planes is interrupted. If the ordering from a certain plane happened to be ABABABA ..., that region would have an HCP structure. There are also intrinsic and extrinsic defects that are layers removed and added respectively. Thus, as the grain edges, the stacking faults are areas of atomic disorder consequently accumulate energy, therefore defects such as precipitates at the grain boundary, disorder atomic (presence of ferritic and martensitic phases) produce a greater reactivity in the crystalline lattice. In the last 60 years, several works have been carried out with different techniques to determinate the SFE, among them are characterization by transmission electron microscopy (TEM) [1,11-17]; X-ray diffraction (XRD) [18-21]; neutron diffraction [16,22]. In the other hand, it has been developed expressions by linear multivariables analysis of experimental data [1, 12, 14, 23-26], and also computational thermodynamics and quantum mechanics first-principles simulations [1, 17, 27-31], including a recently model of a Bayesian neural network (BNN) for the SFE calculation developed by Arpan Das [32]. Yonezawa et al. [1] elaborated several austenitic SS, considering three heat treatments and its manufacture process. They calculated the SFE by TEM characterization of the three heat treatments, which were: solution heat treatment-water cooling (SHTWC), solution heat treatment-furnace cooling (SHTFC), and aging (AGG) tratment. In the order hand, ANN are nonlinear approximations that are based on a fraction of the complex functioning of biological neurons. An artificial neuron receives "inputs" (represent data of any type, whether original or from the outputs of other neurons). This input is transported by a connection with a certain level of "signal strength" (weight). Inside it has a bias value to be adjusted in the same way. The sum of the inputs weighted by the weights $\forall$ the bias value form the activation. This result is known as "activation signal", this is processed by an "activation function" or "transfer function" generating the output of the neuron [32-38]. In the present work a feed forward backpropagation ANN was developed to predict the SFE under given specific ranges of chemical compositions. The characterization data were taken from the Yonezawa´s et al [1] work, for three heat treatment conditions for each SS probe. Different arrangements of neural networks were built to evaluate their performance and find the best arrangement based on the correlation coefficient.

2. METHOD

The first step to build the ANN was to take the selected data from the Yonezawa´s work et al. 2013 [1] and normalize them from 0-1. Subsequently, different ANN architectures were performed to evaluate the performance of the different arrangements. The input layer corresponds to the 33 chemical compositions of the alloys in wt%. One and two hidden layers were evaluated and finally the output layer

corresponds to 99 SFE calculations for the three different heat treatments (SHTWC, SHTFC and AGG). In order to create the ANN, the selected data were stochastically divided as follows: 63, 12 and 12 for training, validation and testing respectively. To complete the ANN development, the 12 last data were simulated for the final validation. Also were evaluated two transfer functions, sigmoid and hyperbolic (figure 1), varying the number of neurons and hidden layers. The different ANN arrangements are shown in figure 2 a-b, figure 3 a-b and figure 4 a-b.

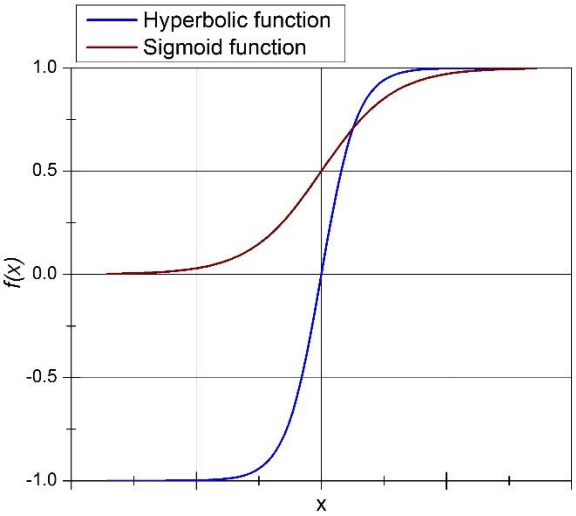

Figure 1. Activation functions

Sigmoid and hyperbolic:

- 10 neurons 1 hidden layer (10N1HL) and 10 neurons 2 hidden layers (10N2HL), show in figure 2 a-b.
- 15 neurons 1 hidden layer (15N1HL) and 15 neurons 2 hidden layers (15N2HL), show in figure 3 a-b.
- 20 neurons 1 hidden layer (20N1HL) and 20 neurons 2 hidden layers (20N2HL), show in figure 4 a-b.

The minimum squared error (*MSE*) is the training error of the model, defined as:

$$MSE = \frac{1}{N}\sum_{i=1}^{N}(Y_i - S_i)^2 \quad (1)$$

Where N is the training number, S_i and Y_i are outputs of the i_{th} output neuron, where S_i and Y_i are the output of the experimental data and the approximated value, respectively [35]. To obtain a faster convergence, the gradient descent method was used and the Levenberg-Marquardt algorithm was selected for this purpose [39-41]. It is very important to mention that only one database was used to avoid calculations with different characterization techniques, linear equations and theoretical approximations by different methods, since if any manufacturing parameter, deformation or characterization technique is altered, the energy is directly affected.

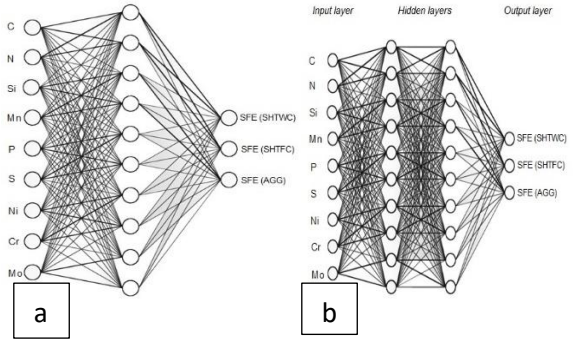

Figure 2. ANN´s architecture. a) 10N1HL. b) 10N2HL.

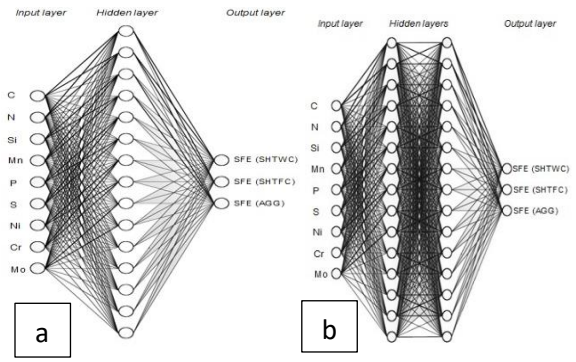

Figure 3. ANN´s architectures. a) 15N1HL; b) 15N2HL.

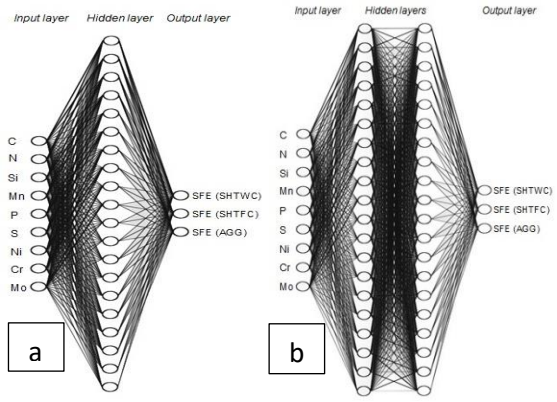

Figure 4. ANN´s architecture. a) 20N1HL b) 20N2HL

To perform the correct supervised training, the input and output data were divided into percentages, of the total available data, 15% was saved for the final simulation. Therefore, the program was trained, validated and tested with the rest, being 100% for the program. This technique is performed to allow the artificial neural network to learn the behavior of the data, without being coupled only to training database. The simulation values are evaluated directly once the weights and biases are set.

- Inside the program:
  - Training: 70%.
  - Validation: 15%.
  - Test: 15%.
- Outside the program:
  - Simulation: 15%.

The aforementioned numerical values for its reproducibility are available in Mendeley repository with the following DOI: 10.17632/t2kr5b4965.1.

3. Results

In the design of this kind of predictive model, one of the most important factors is the performance evaluation of the different architectures of ANN. An evaluation of different architectures of network models was made to observe the performance of each one. Some arrangements were presented (36 neural networks designed), however more models were evaluated. Performance results were obtained for each designed ANN. Figures 5 a-c show the behavior of the prediction using the sigmoid function. Likewise, in figures 6 a-c the results for the networks with hyperbolic function are presented. In these arrangements, the performance was better than the presented in the arrangements with sigmoid function.

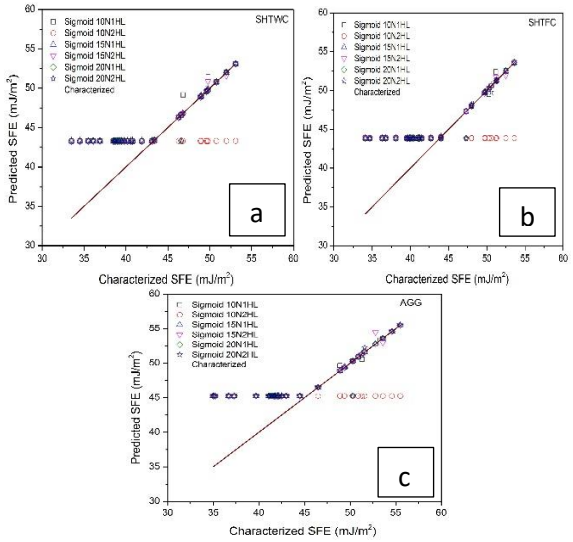

Figure 5. Performance of the sigmoid function in different ANN architectures. a) SHTWC. b) SHTFC. c) AGG.

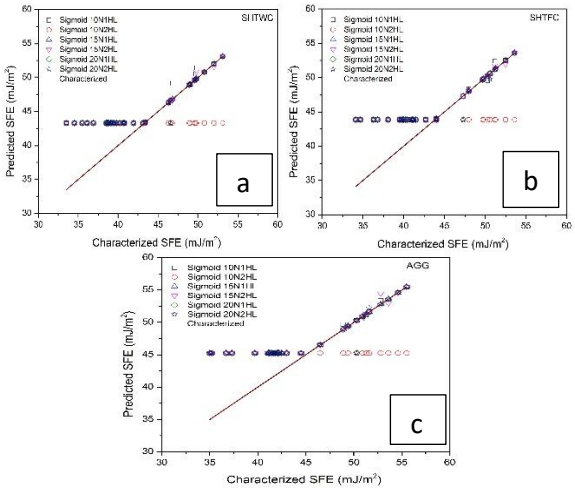

Figure 6. Performance of the hyperbolic function in different ANN architectures. a) SHTWC. b) SHTFC. c) AGG.

Table 1 shows the correlation values obtained for each ANN architecture. It was found that between the 10N1HL and 15N1HL arrangements, the prediction accuracy increases (area highlighted in red in Table 1). Finally, a search was carried out on the aforementioned arrangements, to find the most optimal arrangement based on the number of neurons (complexity for its reproducibility) and correlation coefficient. Therefore, the 12N1HL architecture was selected, shown in Figure 7.

Finally, a comparison of the models was made by multivariable linear equations published by several authors; recent research was taken into account. Figure 8a shows the comparison of the whole the models, including the proposed by Yonezawa et al [1].

Table 1. Coefficient correlation for sigmoid and hyperbolic transfers functions.

ANN architecture	Sigmoid SHTWC	Sigmoid SHTFC	Sigmoid AGG	Hyperbolic SHTWC	Hyperbolic SHTFC	Hyperbolic AGG
10N1HL	0.83	0.83	0.83	0.97	0.97	0.96
10N2HL	0.12	0.01	0.05	0.92	0.93	0.95
15N1HL	0.83	0.83	0.83	0.99	0.99	0.99
15N2HL	0.83	0.83	0.83	0.94	0.96	0.89
20N1HL	0.78	0.78	0.78	0.97	0.97	0.98
20N2HL	0.78	0.78	0.78	0.99	0.98	0.99

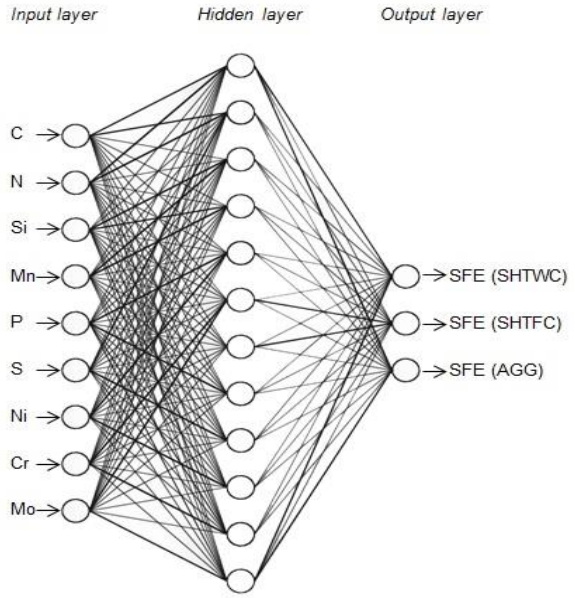

Figure 7. Final ANN architecture selected.

The ANN showed better performance in the prediction capacity is observed. Figure 8b shows a small scale adjustment, for better appreciation, in this image it can be seen that some calculations made by the models previously published diverge with respect to lower or higher energy. This behavior does not show that the models were poorly constructed, instead it is appreciated that when considering the SFE as a numerical data and not as behavior, which is affected by the chemical composition, plastic deformation, heat treatment and characterization technique, any model may fail even including the

ANN designed in this work. The final prediction capacity ranges of the ANN are presented in Table 2, obtaining an excellent field of possibilities to predict.

Table 2. Chemical composition ranges of the ANN.

Chemical composition Wt%	Maximum	Minimum
C	0.075	0.0006
N	0.107	0.001
Si	1.82	0.01
Mn	3.95	0.01
P	0.03	0.004
S	0.0024	0.0002
Ni	19.85	10.8
Cr	24.11	13.09
Mo	2.7	0.04

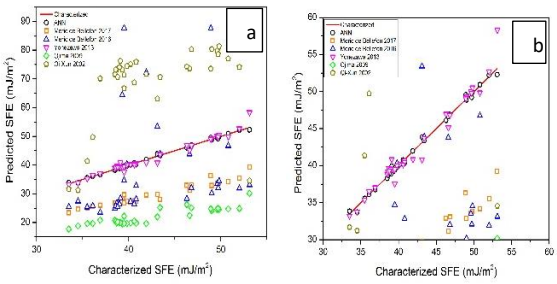

Figure 8. (a) Comparison between the values of SFE characterized and predicted for the SHTWC condition. (b) Adjusted figure from 4a.

4. DISCUSSION

The proposed model can provide a support for the design of austenitic SS, in some cases has special applications. The sample characterization and preparation techniques must be considered to control the dispersion among the difference between the SFE characterized and predicted. It has not been reported a specific influence of this process parameters in the simulation models developed [12, 24-26]. Thus, we propose the design of ANN model based on chemical composition, heat treatment and the TEM as a characterization technique, the latter due to its accuracy in obtaining the dislocation mechanism for the austenitic SS. The model can be considered as an effective general method for the calculation of SFE values, but it is required to carry out further investigations with a specific control of the parameters aforementioned. Currently, artificial intelligence programming does not turn out to be a task with the complication as years before, there are software such as MATLAB that contain interfaces to develop these methods, there are also open codes such as Google's TensorFlow, Microsoft's ONNX and ACUMOS of the Linux foundation projects that allow achieving the same purpose [48-50]. The prediction of SFE by ANN model is a feasible technique for its use in future research and applications for the aforementioned.

5. CONCLUSIONS

A feed forward backpropagation ANN was developed to predict the stacking fault energy in austenitic SS. The database used was compiled from Yonezawa's work. The efficiency obtained in the prediction of the SFE for austenitic SS for three types of heat treatments was R^2=0.99. In addition, the proposed ANN was compared with other models, including Yonezawa's research. The present model shows an improvement in the prediction capability. It was observed in the reported models that the effect of the alloy processes involved affect the SFE values. In order to obtain an effective predictive model it is necessary to build an specific database with

selected chemical composition range under specific heat treatment conditions, sample preparation, plastic deformation percentage and characterization technique.

ACKNOWLEDGMENTS

A. M. Román acknowledges the scholarship support from CONACYT (CVU: 828336) and the technical support of H. H. Hinojosa Galvan, I. Puente, F. Castillo, S. Garcia and G. Aramburo.

REFERENCES

[1] Toshio, Y., Ken, S., Suguru, O., Atsushi H. The Effect of Chemical Composition and Heat Treatment Conditions on Stacking Fault Energy for Fe-Cr-Ni Austenitic Stainless Steel. *Metallurgical and Materials Transactions A* 44 (2013) 5884.

[2] Mumtaz, K., Takahashi, S., Echigoya, J., Kamada, Y., Zhang, L. F., Kikuchi, H., Ara, K., Sato. Magnetic measurements of martensitic transformation in austenitic stainless steel after room temperature rolling. *Journal of Material Science* 39 (2004) 85– 97.

[3] Hamilton, F. G. A., Sheyla, S. C., Pedro, L. N., Ricardo, P. S., Válder, N. F., Paulo, M. O. S., Sérgio, S. M. T. Deformation induced martensite in an AISI 301LN stainless steel: characterization and influence on pitting corrosion resistance *Materials Research* Vol. 10, No. 4, 359-366, 2007.

[4] Amar, K., David C., M., Martin, C. M., John, G. S., David, K. M. Quantitative measurement of deformation-induced martensite in 304 stainless steel by X-ray diffraction. *Scripta Materialia* 50 (2004) 1445–1449.

[5] Peguet, L., Malki, B., Baroux, B. Influence of cold working on the pitting corrosion resistance of stainless steels. *Corrosion Science* 49 (2007) 1933.

[6] Byun, T.S. On the stress dependence of partial dislocation separation and deformation microstructure in austenitic stainless steels. *Acta Materialia* Volume 51, Issue 11, 27 June 2003, Pages 3063-3071.

[7] Byun,T. S., Hashimoto, N., Farrell, K. Temperature dependence of strain hardening and plastic instability behaviors in austenitic stainless steels. *Acta Materialia* Volume 52, Issue 13, 2 August 2004, Pages 3889-3899.

[8] Ernst, F., Cao, Y., Michal, G. M. Heuer, A.H. Carbide precipitation in austenitic stainless steel carburized at low temperature. *Acta Materialia* Volume 55, Issue 6, April 2007, Pages 1895-1906.

[9] Tae-Ho, L., Eunjoo, S., Chang-Seok O., Heon-Young, H., Sung-Joon K. Correlation between stacking fault energy and deformation microstructure in high-interstitial-alloyed austenitic steels. *Acta Materialia* Volume 58, Issue 8, May 2010, Pages 3173-3186.

[10] Shu-XinLi, Yan-NiHe, Shu-RongYu, Peng-YiZhang. Evaluation of the effect of grain size on chromium carbide precipitation and intergranular corrosion of 316L stainless steel. *Corrosion Science* Volume 66, January 2013, Pages 211-216.

[11] Swann, P.R. Dislocation Substructure vs Transgranular Stress Corrosion Susceptibility Of Single Phase Alloys. *Corrosion* 1963, vol. 19, p. 102.

[12] Rhodes, C.G., Thompson, A.W., The composition dependence of stacking fault energy in austenitic stainless

steels. *Metallurgical and Materials Transactions A* 8 (1977) 1901.

[13] Yakubtsov, I. A., Ariapour, A., Perovic, D. D. Effect of nitrogen on stacking fault energy of f.c.c. iron-based alloys. *Acta Materialia* Vol. 47, No. 4, pp. 1271-1279, 1999.

[14] Ojima, M., Adachi, Y., Tomota, Y., Katada, Y., Kaneko, Y., Kuroda, K., Saka, H. Weak Beam TEM Study on Stacking Fault Energy of High Nitrogen Steels. *Steel Research International* 80 (2009) 477.

[15] Pierce, D., Bentley, J.,Jimenez, J., Wittig, J. Stacking fault energy measurements of Fe–Mn–Al–Si austenitic twinning-induced plasticity steels. *Scripta Materialia* 66 (2012) 753.

[16] Lee, T.H., Ha, H.Y., Hwang, B., Kim, S.J., Shin, E. Effect of Carbon Fraction on Stacking Fault Energy of Austenitic Stainless Steels. *Metallurgical and Materials Transactions A*, 2012, vol. 43A, p. 4455.

[17] Lu, J., Lars H., Erik H., Karin H. A., Mikael, G., Wei L., Levente, V., Ardeshir, G. tacking fault energies in austenitic stainless steels. *Acta Materialia* 111, 1 June 2016, 39.

[18] Smallman, R.E., Westmacott, K.H. Stacking faults in face-centred cubic metals and alloys. *The Philosophical Magazine: A Journal of Theoretical Experimental and Applied Physics* 1957, vol. 2, p. 669.

[19] Reed, R.P., Schramm, R.E. Relationship between stacking-fault energy and x-ray measurements of stacking-fault probability and microstrain. *Journal of Applied Phyics*. 45 (1974) 4705.

[20] Huang, S.K., Wen, Y.H., Li, N., Teng, J., Ding, S., Xu, Y. G. Application of damping mechanism model and stacking fault probability in Fe–Mn alloy. *Materials Characterization* 59, Issue 6, June 2008, 681.

[21] Moallemi, M., Hanzaki, A.Z., Mirzaei, A. On the Stacking Fault Energy Evaluation and Deformation Mechanism of Sanicro-28 Super-Austenitic Stainless Steel. *Journal of Materials Engineering and Performance* 2015, vol. 24, p. 2335.

[22] Kang, M., Woo, W., Lee, Y.-K., Seong, B.-S. Neutron diffraction analysis of stacking fault energy in Fe–18Mn–2Al–0.6C twinning-induced plasticity steels. *Materials Letters* 76 (2012) 93.

[23] Schramm, R.E., Reed, R.P. Stacking fault energies of seven commercial austenitic stainless steels. *Metallurgical and Materials Transactions A* 6 (1975) 1345.

[24] Qi,X., An-Dong, W., Xiao-Nong, C., Xin-Min, L., Stacking fault energy of cryogenic austenitic steels. *Chinese Physics* 11 (2002) 596.

[25] Meric de Bellefon, G., Domain, C., van Duysen, J. C., Sridharan, K. *Conference Paper · April 2016*.

[26] Meric de Bellefon, G., van Duysen, J.C., Sridharan, K. Composition-dependence of stacking fault energy in austenitic stainless steels through linear regression with random intercepts. *Journal of Nuclear Materials* 492 (2017) 227.

[27] Olson, G.B., Cohen, M. A general mechanism of martensitic nucleation: Part I. General concepts and the FCC → HCP transformation. *Metallurgical and Materials Transactions A* 1976, vol. 7,p. 1897.

[28] Vitos, L., Nilsson, J., Johansson. B. Alloying effects on the stacking fault energy in austenitic stainless steels from first-principles theory. *Acta Materialia* 54 (2006), 3821.

[29] Lu, S., Hu, Q.M., Johansson, B., Vitos, L. Stacking fault energies of Mn, Co and Nb alloyed austenitic stainless steels. *Acta Materialia* 59 (2011) 5728.

[30] Geissler, D., Freudenberger, J., Kauffmann, A., Martin, S., Rafaja, D.

Assessment of the thermodynamic dimension of the stacking fault energy. *Philosophical Magazine* 2014, vol. 94, p. 2967.

[31] Pierce, D., Jimenez, J., Bentley, J., Raabe, D., Oskay, C., Wittig, J. The influence of manganese content on the stacking fault and austenite/ε-martensite interfacial energies in Fe–Mn–(Al–Si) steels investigated by experiment and theory. *Acta Materialia* 68 (2014) 238.

[32] Das, A. Revisiting Stacking Fault Energy of Steels. *Metallurgical and Materials Transactions A* 47 (2015) 748.

[33] Chiappetta, P., Colangelo, P., De Felice, P., Nardulli, G., Pasquariellod, G. Higgs search by neural networks at LHC. *Physics Letters B*, Volume 322, Issue 3, 17 February 1994, 219-223.

[34] Amr, R., Samy, K. H. *IntechOpen Applying Artificial Neural Networks*, DOI: 10.5772/51273, 2013.

[35] Saeed, S., Rouein, H., Shokoufe, T., Alimorad, R. Neural network and genetic algorithm for modeling and optimization of effective parameters on synthesized ZSM-5 particle size. *Materials Letters* 136 (2014) 138.

[36] Yetim, A.F., Codur, M.Y., Yazici, M. Using of artificial neural network for the prediction of tribological properties of plasma nitrided 316L stainless steel. *Materials Letters* 158 (2015) 170.

[37] Baldi, P., Sadowski, P., Whiteson, D. Searching for exotic particles in high-energy physics with deep learning. *Nature communications*. doi: 10.1038/ncomms5308.

[38] Jiménez-Come, M. J., Turias, I. J., Ruiz-Aguilar, J. J., Trujillo, F. Characterization of pitting corrosion of stainless steel using artificial neural networks. *Journal of Materials and Corrosion* 2015, 66, No. 10 1084.

[39] Marquardt, D. W. An Algorithm for least-squares estimation of nonlinear parameters *Journal of the Society for Industrial and Applied Mathematics*. 1963, Vol. 11, No. 2, 431.

[40] Hagan, M.T., Menhaj, M.B. Training feedforward networks with the Marquardt algorithm. IEEE *Transactions of Neural Networks* Volume: 5, Issue: 6, Nov 1994, 989.

[41] Martin T. H., Howard, B. D., Mark, H. B., Orlando, J. *Neural network design*., Chapters 10,12., ISBN 0971732116, 9780971732117.

[42] Ponce, P. Inteligencia artificial con aplicaciones a la ingeniería., *Alfaomega Grupo Editor, S.A. de C.V., México*., ISBN: 978-607-7854-83-8.

[43] Petrov, N.Y., Yakubtsov, I.A. Thermodynamic Calculation of Stacking Fault Energy and its Effect on Fcc→Hcp Phase Transformation in Nitrogen Alloyed Stainless Steels. *Materials Science Forum* 1990, vol. 8, p. 889.

[44] Simmons, J.W. Overview: high-nitrogen alloying of stainless steels. *Materials Science and Engineering A* 1996, vol. 207, p. 159.

[45] Prokoshkina, V., Kaputkina, L. *Materials Science Engineering A*, 2008, vols. 481–482, p. 762.

[46] Bracke, L., Penning, J., Akdut, N. The Influence of Cr and N Additions on the Mechanical Properties of FeMnC Steels. *Metallurgical and Materials Transactions A*, 2007, vol. 38A, p. 520.

[47] Yang, J.H., Wayman, M. Self-accomodation and shape memory mechanism of ϵ-martensite—I. Experimental observations. *Material Characterization*, 1992, vol. 28 (1), p. 23.

[48] https://www.tensorflow.org/ last accessed 04/25/2018

[49] https://onnx.ai/ last accessed 04/25/2018

[50] https://www.acumos.org/ last accessed 04/25/2018

Acerca de los autores

Alfonso M. Román es Ingeniero Mecánico, egresado de la Facultad de Ciencias Químicas e Ingeniería, Universidad Autónoma del Estado de Morelos. Actual estudiante de maestría en el Centro de Investigación en Ingeniería y Ciencias Aplicadas, UAEM. Algunas áreas de interés: ciencia de materiales, diseño de materiales protésicos, aplicación de tecnología aditiva al área biomecánica y energía e inteligencia artificial.

Bernardo Campillo es Dr. en química metalúrgica, egresado de la Universidad Nacional Autónoma de México. Actual investigador del Instituto de Ciencias Físicas y coordinador de posgrado de la Facultad de Química de la UNAM en el Instituto de Ciencias Físicas. Algunas áreas de interés: Ciencia de materiales, plasma a baja temperatura, materiales intermetálicos, tratamientos térmicos y técnicas espectroscópicas.

Arturo Molina es Dr. en ingeniería, egresado de la Universidad Nacional Autónoma de México. Profesor-Investigador del Centro de Investigación en Ingeniería y Ciencias Aplicadas, UAEM. Áreas de interés: análisis de microestructuras, propiedades mecánicas, procesos termo-mecánicos, tratamientos térmicos, metalurgia de polvos y aleado mecánico.

Horacio Martínez es Dr. en física, egresado de la Facultad de Ciencias, Universidad Nacional Autónoma de México (UNAM). Investigador del Instituto de Ciencias Físicas, UNAM, jefe del laboratorio de espectroscopia. Algunas áreas de interés: fenómenos de plasma, plasma a bajas temperaturas, modificaciones de material protésico mediante plasma, y técnicas espectroscópicas.

Itzel Reyes es Ingeniera Química Metalúrgica, egresada de la Facultad de Química, Universidad, Nacional Autónoma de México. Profesora de la F.Q. (UNAM) y estudiante de maestría en Metalurgia. Algunas áreas de interés: Ciencia de materiales, técnicas de caracterización de materiales, (SEM, EBSD, TEM, Absorción atómica, AFM, XRD), materiales intermetálicos y corrosión.

Osvaldo Flores es Dr. en Ing. Química Metalúrgica, egresado de la Universidad Nacional Autónoma de México. Actualmente en el Instituto de Ciencias Físicas y profesor de posgrado de la Facultad de Química de la UNAM. Algunas áreas de interés: Ciencia de materiales, plasma a baja temperatura, hidrogeno en metales, materiales intermetálicos, tratamientos térmicos, técnicas espectroscópicas, tecnología aditiva al área biomecánica y energía, y diseño de materiales protésicos.